Int. J. Electrochem. Sci., 7 **(2012)** 11001 - 11010

International Journal of
ELECTROCHEMICAL
SCIENCE
www.electrochemsci.org

Effect of Sb_2O_3 Modification on Electrochemical Performance of $LiMn_2O_4$ Cathode Material

Yulin Ma, Yunzhi Gao, Pengjian Zuo, Xinqun Cheng, Geping Yin[*]

School of Chemical Engineering and Technology, Harbin Institute of Technology, Heilongjiang 150001, PR China
[*]E-mail: myl510@yahoo.com.cn; yingphit@hit.edu.cn

Received: 18 September 2012 / *Accepted:* 10 October 2012 / *Published:* 1 November 2012

Sb_2O_3-coated $LiMn_2O_4$ is prepared by chemical precipitation method to improve the cycling stability of $LiMn_2O_4$. The uncoated and Sb_2O_3-coated $LiMn_2O_4$ materials are characterized by the X-ray diffraction (XRD), Transmission electron microscope (TEM) and X-ray photoelectron energy spectrum (XPS). The results indicate that the crystal structure of $LiMn_2O_4$ is not affected by the Sb_2O_3 coating but lattice constant has changed, and most Sb_2O_3 coat on $LiMn_2O_4$ surface. Electrochemical test shows that Sb_2O_3-coating could improve the cycling performance of $LiMn_2O_4$. At room temperature, the capacity retention of 2.0 wt. % Sb_2O_3-coated material is 93.5% after 60 cycles while that of the bare sample is only 86.3%. Electrochemical impedance spectroscopy (EIS) demonstrates that the improved performance of the Sb_2O_3-coated $LiMn_2O_4$ is due to suppress the augment of charge transfer resistance during cycling, which indicates that the coating decreases the surface reaction between cathode and electrolyte. Data from TG-DSC studies show that the thermal stability of the surface modified $LiMn_2O_4$ electrode is improved.

Keywords: Lithium ion battery, $LiMn_2O_4$ cathode, Surface modification, Coatings.

1. INTRODUCTION

In recent years, the demand for power batteries with higher energy and power capability becomes urgent as the decrease of worldwide energy. Lithium ion batteries are considered as the promising candidate for the future mobile energy supply. Concerning cathode materials of lithium ion batteries, spinel $LiMn_2O_4$ has been the attractive candidate for electric vehicles due to the cheap, abundant, and environmental friendly features. However, $LiMn_2O_4$ displays fast capacity fading during cycles especially at elevated temperatures due to the following factors[1-4]: (1) the dissolution of manganese-ions; (2) the Jahn-Teller effect especially in deeply discharged $Li_xMn_2O_4$; (3) the

electrochemical oxidation of the organic electrolyte at the charged state. It is generally thought that the most important reason was the dissolution of Mn ions [5-8]. The dissolution can be attributed to the HF generated during cycles in $LiFP_6$-based electrolyte. On the other hand, safety issue is one of the biggest barriers for the development of large-sized lithium-ion batteries，so the materials must have higher safety.

To improve the cycling performance of $LiMn_2O_4$, much attention has been focused on surface coating with metal oxides, such as Li_2O_3 [9], MgO[10], Al_2O_3[11], ZnO[12], Co_3O_4[13], ZrO_2[14], CeO_2[15] and TiO_2[16]. After coating, the coating layer can reduce the contact area of $LiMn_2O_4$ electrode/electrolyte interface and partly suppress the dissolution of the Mn ions from the spinel into the electrolyte. Furthermore, the phase transition during charge-discharge process was suppressed and the lattice distortion of the spinal $LiMn_2O_4$ especially at higher temperature was reduced. Recently, Sb_2O_3 is reported to be able to improve the electrochemical performance and thermal safety of $Li_{1.1}CoO_2$[17]. Nevertheless, the modified $LiMn_2O_4$ by Sb_2O_3 has not been reported. In addition, Sb_2O_3 is a commonly used flame retardant material. Thus, we hope that the Sb_2O_3 modification not only improve the cycling performance but also improve the safety of materials.

In this paper, Sb_2O_3 is coated on the surface of $LiMn_2O_4$ powders by chemical precipitation method. The effect of Sb_2O_3 coating on the electrochemical performance at the room and elevated temperatures is investigated and the mechanism of improved performance is discussed.

2. EXPERIMENTAL

2.1 Synthesis of Sb_2O_3-coated $LiMn_2O_4$

$LiMn_2O_4$ was prepared by calcining a stoichiometric mixture of lithium carbonate, electrolytic manganese dioxide at 750°C for 12 h in air, followed by slow cooling to the ambient temperature. The precursor of Sb_2O_3-coated $LiMn_2O_4$ material was synthesized by dropping the ethanol solution of antimony trichloride the buffer solution made of sodium hydroxide, triethanolamine and $LiMn_2O_4$ powder. The precursor was vacuum dried under 150°C to obtain the Sb_2O_3-coated $LiMn_2O_4$ material. The expected amounts of Sb_2O_3 were about 1, 2 and 3.0 wt. % of the $LiMn_2O_4$ powders.

2.2 Characterization of Sb_2O_3-coated $LiMn_2O_4$

To investigate the crystal structure, the prepared powder was analyzed by Powder X-ray diffraction (XRD) method using a D/Max-rB diffract meter equipped with Cu Kα radiation in the range of $2\theta = 10\text{-}90°$ and the step size was 0.02°. The surface morphologies of the pristine and Sb_2O_3-coated powder were observed by transmission electron microscopy (TEM, HITACHI S-7650). The surface properties of the pristine and Sb_2O_3-coated $LiMn_2O_4$ were analyzed by X-ray photoelectron spectroscopy (XPS, PHI5700-ESCA) which were performed on a Physical Electronics Quantum-5600 Scanning ESCA Microprobe with Al Kα (1486.7 eV) .

The thermal stability of $LiMnO_2$ powder was investigated by differential scanning calorimetry combined with thermogravimetry (STA449F3, Netzsch). The cells were pre-cycled for three cycles with 0.1mA/cm^2 to reach a stable capacity level and the cycling was interrupted when the cells were charged to a fully intercalated state (4.3V). Then the charged cells were disassembled in a glove box. The test powder was scraped from electrode after remove the electrolyte. A given amount of fresh electrolyte solution and test electrode powder was sealed in a hermetic pan. All of the experiments above were conducted under an argon atmosphere. The pan was heated from room temperature to 400 °C at 5°C min^{-1}.

2.3 Electrochemical measurements of Sb_2O_3-coated $LiMn_2O_4$ cathode materials

The cathode electrodes with a diameter of 1.4 cm were prepared by mixing active material, acetylene black and polyvinylidene fluoride (PVDF) (8:1:1, by weigh) dissolved in N-methylpyrrolidnone (NMP) to form slurry, which was then coated on Al foil and dried at 120 °C for 14 h. The pure Sb_2O_3 electrode was prepared with the similar method of $LiMn_2O_4$ electrode in order to investigate the activity of the Sb_2O_3. The 2025-type coin cells were assembled in a glove box filled with high pure argon. A metal lithium foil and a solution of 1.0mol/L $LiPF_6$ EC: DEC: DMC (1:1:1) were used as the anode and the electrolyte, respectively. The charge-discharge tests of the cells were tested between 3.0V and 4.30 V (at 0.2C) on a battery testing system (Neware BTS) at 25°C and 55°C. The cyclic voltammetry (CV) tests were performed on a CHI604B electrochemical workstation with a scan rate of 0.5 mV s^{-1}. The electrochemical impedance spectroscopy (EIS) analysis was also carried out on CHI604B electrochemical workstation using a tri-electrode cell to investigate the variation of cell resistances at different cycle stages. The tests were performed in the frequency range of 100 kHz to 0.01Hz using a voltage vibration of 5mV.

3. RESULTS AND DISCUSSION

Fig. 1 shows the X-ray diffraction patterns of pristine $LiMn_2O_4$ and Sb_2O_3 coated $LiMn_2O_4$. No obvious difference is detected in X-ray diffraction patterns of pristine and Sb_2O_3-coated $LiMn_2O_4$. All compounds are identified as well-defined single phase products in the face-centered cubic spinel structure with an *Fd*3*m* space group, in which the lithium-ions occupy the tetrahedral (8a) sites and metal ions reside at the octahedral (16d) sites. This suggests that the crystal structure of $LiMn_2O_4$ is not affected by the Sb_2O_3 coating. The absence of Sb_2O_3 phases in the entire range of the diffraction patterns may be due to the very low concentrations of antimony. However, there is a slight decrease in the lattice constant of 8.225, 8.223, 8.219 and 8.212, corresponding to the 0%, 1%, 2%, and 3% Sb_2O_3 coated $LiMn_2O_4$, respectively. According to Zhan [17], Sb can dope into the $Li_{1.1}CoO_2$ by replacing Co and retain the spinel structure α-$NaFeO_2$ type structure. In addition, Guo [18] reported that the lattice constant of $LiNi_{0.5}Co_{0.25}Mn_{0.25}O_2$ was slightly smaller than those for the ZnO_2-coated $LiNi_{0.5}Co_{0.25}Mn_{0.25}O_2$ sample. They explained that the radius of Zn is larger than that of other elements

in this material and the solid solution layer of Li-Ni-Co-Mn-Zn-O was formed on the surface of $LiNi_{0.5}Co_{0.25}Mn_{0.25}O_2$ sample. The similar surface reactions happen in the TiO_2-coated $LiMn_2O_4$ [16] and the Al_2O_3-coated $LiCoO_2$[19] . In this experiment, the radius of Sb^{3+} (0.076nm) is smaller than that of Mn^{2+} (0.080nm). Therefore, we propose that antimony maybe doped into the spinel $LiMn_2O_4$ by replacing Mn and retained the spinel structure, which means a little solid spinel compound of $LiSb_xMn_{2-x}O_4$ formed on the surface of spinel $LiMn_2O_4$ during the synthetical process and caused the shrinkage of the lattice.

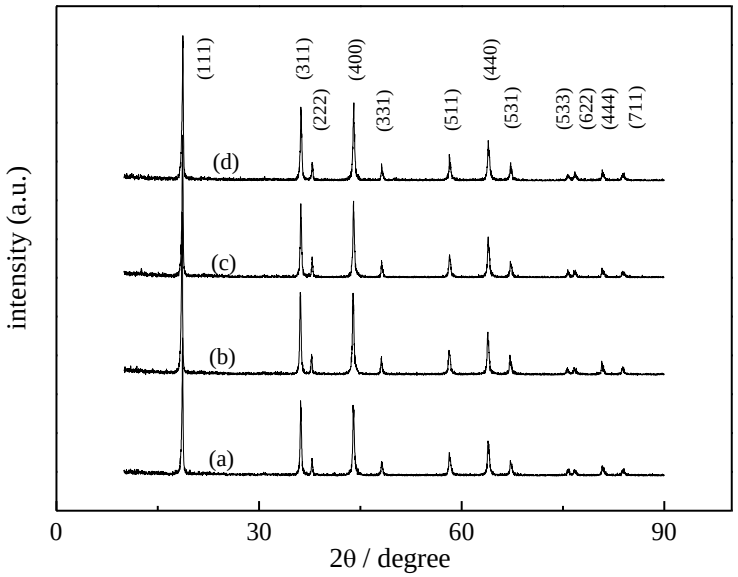

Figure 1. XRD patterns of 0 % (a), 1 % (b), 2 % (c) and 3 % (d) Sb_2O_3-coated $LiMn_2O_4$

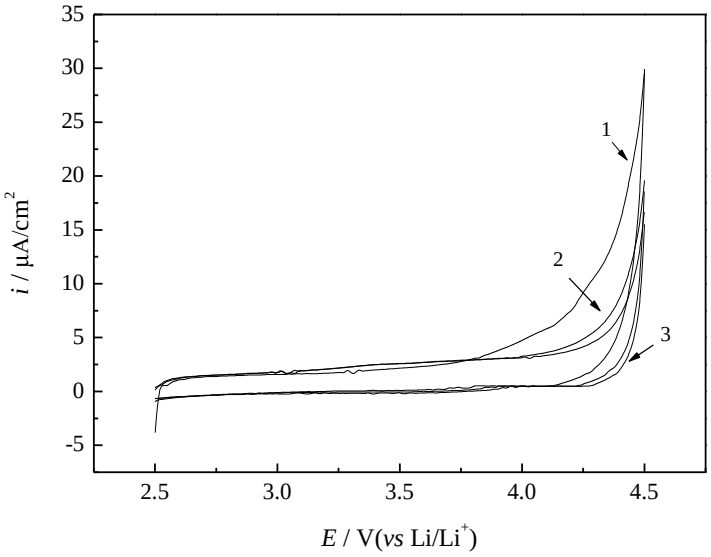

Figure 2. CV curves of Sb_2O_3

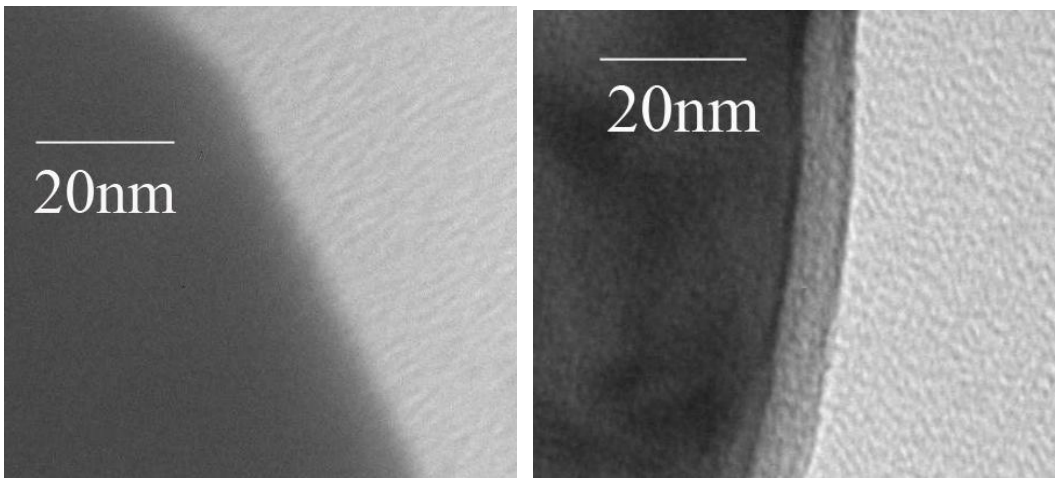

Figure 3. TEM images of the pristine (a) and 2 % Sb_2O_3-coated $LiMn_2O_4$ (b)

Fig.2 shows the CV curves of the pure Sb_2O_3 electrode. From Fig. 2, the oxidative peak occur after 4.0V and the value of the oxidative current is about 10^{-6}A. Compared to the value of the oxidative current of $LiMn_2O_4$ (10^{-3}A), the current is so small that we think Sb_2O_3 is inactive. Fig. 3 exhibits the TEM images of pristine (a) and 2 % Sb_2O_3-coated $LiMn_2O_4$ (b). As expected, it is clearly observed that a layer with the thickness of 8 nm was coated on the surface of $LiMn_2O_4$.

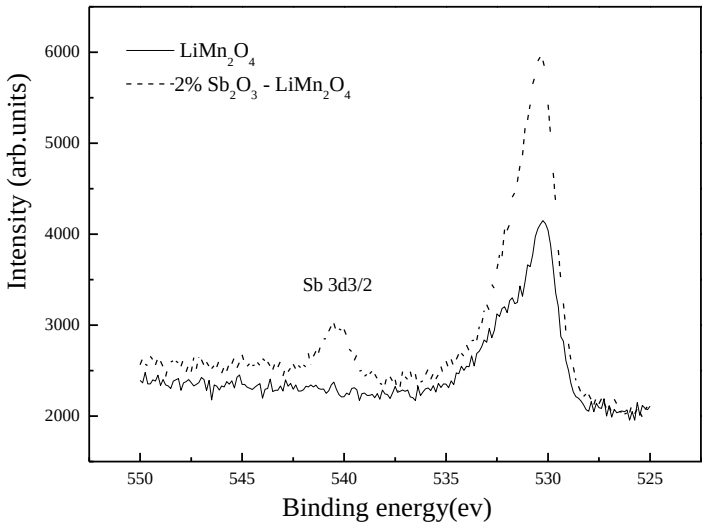

Figure 4. The Sb3d3/2 XPS spectra of the surface of the pristine $LiMn_2O_4$ (solid line) and 2% Sb_2O_3-coated $LiMn_2O_4$ (dash line)

XPS is an effective method to provide the elemental oxidation states analysis of the surface film[20,21]. Thus, the surface of the 2 % Sb_2O_3-coated $LiMn_2O_4$ electrodes was detected by XPS. Fig. 4 shows the XPS spectra of the pristine and 2 % Sb_2O_3-coated $LiMn_2O_4$. As can be seen, in the spectra

of 2 % coated $LiMn_2O_4$, an obvious peak occurs at 540 eV which can be contributed to the Sb3d3/2 of Sb_2O_3[22,23], while there is no peak at 540 eV in the pristine $LiMn_2O_4$. It can be speculated from the XPS spectra that the Sb_2O_3 exist in the surface of Sb_2O_3-coated $LiMn_2O_4$. Associated with the results of XRD, we suppose that two kinds of antimony compound, Sb_2O_3 and $LiSb_xMn_{2-x}O_4$ all exist on the surface of modified $LiMn_2O_4$.

Fig. 5 shows the charge-discharge curves of the pristine and Sb_2O_3-coated $LiMn_2O_4$ performed during cycles at room temperature and high temperature. From Fig. 5a, the initial discharge capacity of the coated materials is lower than that of the pristine $LiMn_2O_4$ and decrease with the increase of Sb_2O_3, which is similar to other oxide-coated cathodes [24,25]. The initial discharge capacities of pristine $LiMn_2O_4$, 1 %, 2 % and 3 % Sb_2O_3 coated $LiMn_2O_4$ are 116.4 mAh g^{-1}, 115.7 mAh g^{-1}, 115.1 mAh g^{-1} and 113.5 mAh g^{-1}, respectively. On the other hand, the capacity of pristine material declines to 96.6 mAh g^{-1} after 60 cycles, which shows the capacity loss of 13.7 %. By contrast, the coated $LiMn_2O_4$ exhibits small capacity loss, especially 2% coated material (only 6.5%). The cycle stability is significantly improved by Sb_2O_3 coating. The decrease of the initial discharge capacity of coated materials is mainly caused by the inactive Sb_2O_3.

The cycling performance of pristine and 2 % Sb_2O_3 coated-$LiMn_2O_4$ at 55°C between 3.0V and 4.3V are illustrated in Fig.5b. As can be seen, the Sb_2O_3 coating can significantly reduce the capacity fading of $LiMn_2O_4$ at elevated temperature. The uncoated-$LiMn_2O_4$ delivers a discharge capacity of 110.8 mAh g^{-1} at the first cycle and remains only 87.7 mAh g^{-1} after 20 cycles with the capacity loss of 20%. While under the same conditions, 12.6 % capacity loss is found for 2% Sb_2O_3 coated $LiMn_2O_4$. These results obviously suggest that the surface modification of $LiMn_2O_4$ spinel with Sb_2O_3 is effective to reduce capacity fading of $LiMn_2O_4$ at elevated temperature.

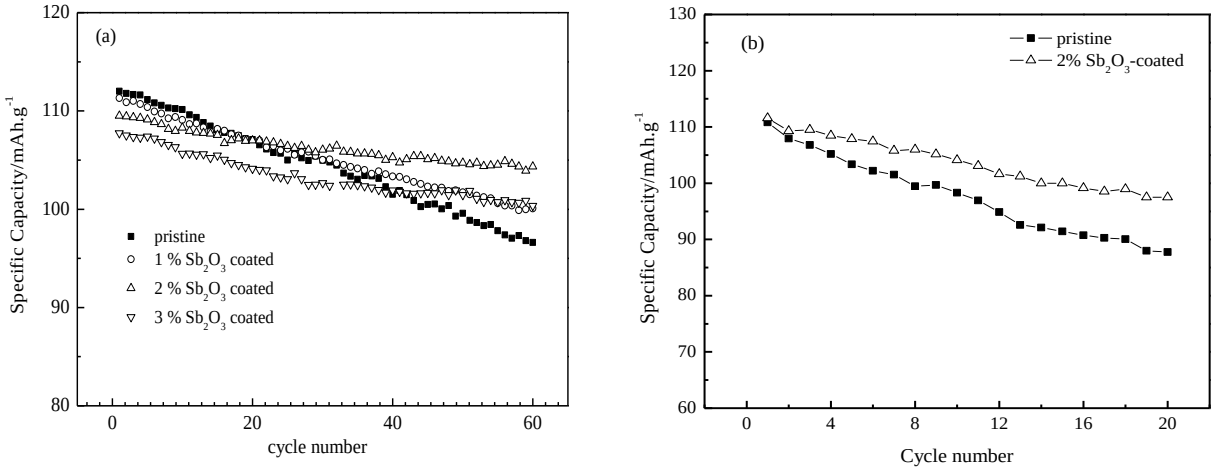

Figure 5. Discharge capacities of pristine and Sb_2O_3-coated $LiMn_2O_4$ cathodes at the range of 3.0-4.3V with a constant current density of 0.2C at 25°C (a) and 55°C (b)

In order to understand the mechanism of improved cycling performance of Sb_2O_3 coated-$LiMn_2O_4$, we investigated the stability of Sb_2O_3 during cycle process. Fig.6 shows the Sb3d3/2 XPS spectra of 2% Sb_2O_3-coated $LiMn_2O_4$ after 30 cycles. The peak of Sb3d3/2 still exists at 540.0

ev[22,23], which is in accordance with fresh sample. These results imply that the Sb_2O_3 on the surface of the $LiMn_2O_4$ particle has good stability. Combined with the TEM, we supposed that the coating layer and the surface solid solution layer can reduce the contact area of $LiMn_2O_4$ electrode/electrolyte interface and partly suppress the dissolution of the Mn ions from the spinel into the electrolyte.

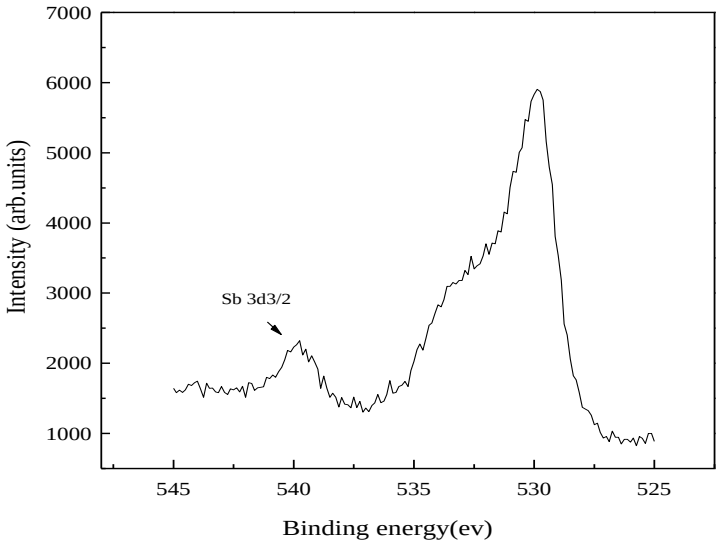

Figure 6. The Sb3d3/2 XPS spectra of the surface of the 2% Sb_2O_3-coated $LiMn_2O_4$ after 30 cycles

The electrode/electrolyte interface is another important factor on the electrochemical performance of $LiMn_2O_4$ except for the structure stability of the cathode materials. EIS was measured to investigate the kinetics of Li^+ insertion/desertion into the pristine and Sb_2O_3 coated $LiMn_2O_4$. Fig. 7 shows the Nyquist plots of bare and Sb_2O_3-modified $LiMn_2O_4$ after different cycles. Both spectra have the high frequency semicircles, the middle frequency semicircles and the low frequency tails. The impedance spectra were fitted with the equivalent circuit model (insert in Fig. 7a.). As other models[18,26-27], this model also consist of Li^+ migration through the surface film, charge-transfer through the electrode-electrolyte interface and the solid-state diffusion of Li^+ in the material. In this circuit, Rs denotes the ohmic resistance, R_f and CPE1 are the surface film resistance and film capacitance, Rct and CPEdl are charge transfer resistance and double layer capacitance at the electrolyte-electrode interface, and W represents the diffusion impedance, respectively. From Fig. 7a, the $LiMn_2O_4$ cathode and Sb_2O_3-modified $LiMn_2O_4$ cathode have similar EIS after the second cycle, which indicates that two kinds of cathode have analogous kinetic character. However, there is the obvious difference in Fig. 7b. The parameters of the equivalent circuit obtained from computer simulations are shown in Table 1. It can be seen that the Rct of pristine $LiMn_2O_4$ increases from 13.0Ω to 36.1Ωand the coated sample only increases from 15.0Ω to 29.2Ω. Obviously, the Sb_2O_3 coating can suppress the augment of charge transfer resistance during cycle process, which cause a better cycle stability of the Sb_2O_3 coated $LiMn_2O_4$ than the pristine sample.

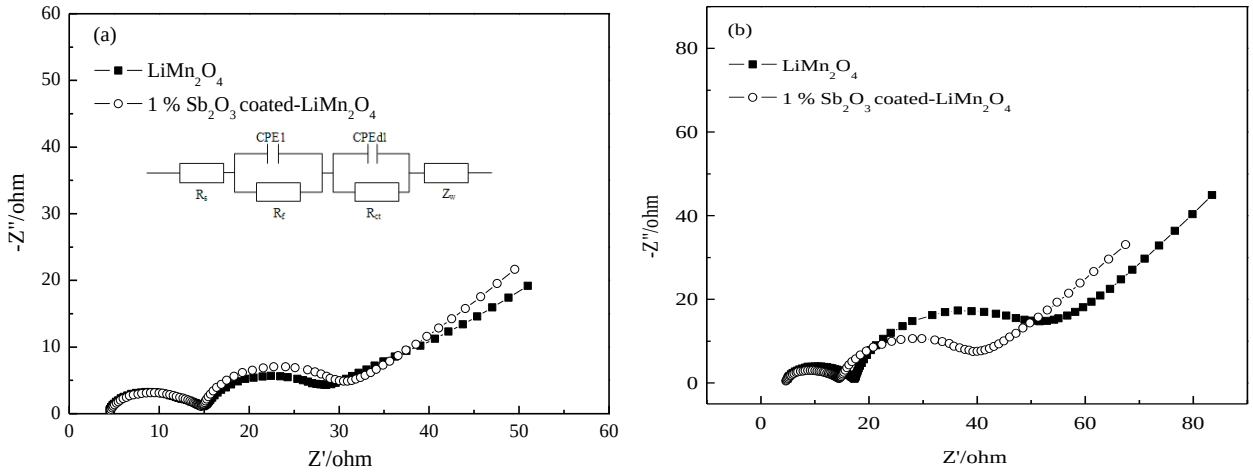

Figure 7. Electrochemical impedance spectroscopy of the electrodes after 2 cycle (a) and 30 cycles(b)

Table 1. Simulated impedance parameters using the equivalent circuit

	Pristine		1% Sb_2O_3	
	2th	30th	2th	30th
Rs (Ω)	5.07	4.95	4.67	4.71
Rf (Ω)	11.5	13.0	10.1	11.3
Rct (Ω)	13.0	36.1	15.0	19.0

Fig. 8 shows the TG-DSC profiles of $LiMn_2O_4$ and 2%Sb_2O_3 coated $LiMn_2O_4$ in charged state with fresh electrolyte. TG profiles show that the weight of each crucible was constant, indicating that no leakage was occurred during experiments. DSC curve of pristine $LiMn_2O_4$ obviously shows three exothermic reactions from 210◦C to 330◦C. 2%Sb_2O_3 coated $LiMn_2O_4$ exhibits a small hump around 175℃ and then slowly generates heat from 210◦C. The estimated total heat generation of pristine $LiMn_2O_4$ is 470 $w \cdot g^{-1}$ while the 2%Sb_2O_3 coated $LiMn_2O_4$ shows a lower heat of 240 $w \cdot g^{-1}$, which is 49% less than that of pristine $LiMn_2O_4$. It is expected that the coating not only reduces the direct contact between electrolyte and active materials, but also stabilizes the surface structure of active material, which thus inhibits the oxygen from active materials and then finally increases the thermal stability of the active materials. On the other hand, Sb_2O_3 itself is a usual inorganic flame retardants, which can react with trace HF in the electrolyte and generate a new gas phase on the electrode surface at high temperatures, so as to further separate the electrolyte and the electrode, reducing the reaction heat between the electrolyte and the electrode.

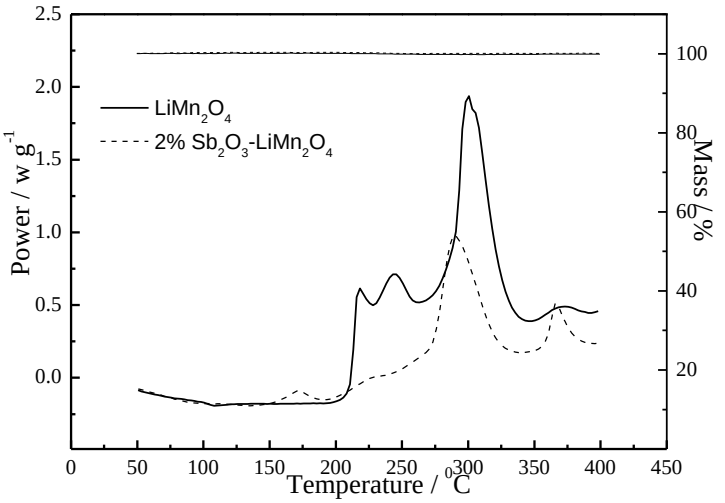

Figure 8. TG-DSC profiles of charged $LiMn_2O_4$ and Sb_2O_3 coated $LiMn_2O_4$ with electrolyte

4. CONCLUSION

Sb_2O_3 was coated on surface of $LiMn_2O_4$ by chemical precipitation method. The initial discharge capacity was decreased with the increase of Sb_2O_3 content. Compared to the other proportion samples, 2% Sb_2O_3-coated $LiMn_2O_4$ sample exhibited slightly decrease of original specific capacity but maintained excellent capacity retention. The Sb_2O_3 coating reduced the contact area of $LiMn_2O_4$ electrode/electrolyte interface and suppressed the augment of charge transfer resistance during cycling, which guaranteed the enhanced electrochemical performance of Sb_2O_3-coated $LiMn_2O_4$. At the same time, the thermal stability of $LiMn_2O_4$ was improved by Sb_2O_3 coating.

ACKNOWLEDGMENTS

We express our appreciation for the support from the National Natural Science Foundation of China (No. 51202047), the Fundamental Research Funds for the Central Universities (No. HIT. NSRIF. 2011022) and the Heilongjiang Postdoctoral Fund (LBH-Z11141).

References

1. R.J. Cummow, A.D. Kock and M.M. Thackeray. *Solid State Ionics*. 69 (1994) 59.
2. A.D. Robertson, S.H. Lu, W.F. Acerill and J.R. Howard. *J. Electrochem. Soc*. 144 (1997) 3500.
3. G.G. Amatucci, N.Pereira, T. Zheng, I. Plits and J.M. Tarascon. *J. Power Sources*. 81- 82 (1999) 39.
4. Y. Xia and M. Yoshio. *J. Power Sources*. 66(1-2) (1997) 129.
5. M.M Wohlfahrt, C.Vogler and J. Garche. *J. Power Sources*. 127 (2004) 58.
6. T. Inoune and M. Sano. *J. Electrochem. Soc*. 145 (1998) 3704.
7. L.J. Fu, H. Liu, C. Li, Y.P. Wu, E. Rahm, R. Holze and H.Q. Wu. *Solid State Sciences*. 8 (2006) 113.
8. T. Erikssom, T. Gustafasson and J.O. Thomas. Electrochem. *Solid-State Lett.* 5 (2002) A35.
9. L.J. Feng, S.P. Wang, X.Y.Qin, H.Y. Wei and Y.Z.Yang. *Materials Lett*. 78 (2012) 116.

10. J. S. Gnanaraj, V. G. Pol, A. Geranken and D. Aurbach. *Electrochem. Comm*., 5 (2003) 940.
11. W. K. Kim, D. W. Han, W. H. Ryu, S. J. Lim and H.S. Kwon. *Electrochim. Acta*. 71 (2012) 17.
12. D.Q. Liu, X. Q. Liu and Z. Z. He. *J. Alloys and Comp*. 436 (2007) 387.
13. J. Cho, T. J. Kim, Y. J. Kim and B. Park. *Chem. Comm*., 12 (2001) 1074.
14. Y.M. Lin, H.C.Wu, Y.C.Yen, Z. Z. Guo, M. H. Yang, H.M,Chen, H. Sheu and N. Wu. *J. Electrochem. Soc*., 152 (2005) A1526.
15. H.Ha, N. Yun and K.Kim. *Electrochim. Acta*. 52 (2007) 3236.
16. L.H.Yu, X.P.Qiu, J.Y.Xi, W.T.Zhu and L.Q.Chen. *Electrochim. Acta*. 51 (2006) 6406.
17. J.P.Yu, X.H.Hu, H.Zhan and Y.H.Zhou. *J. Power Sources*. 189 (2009) 697.
18. R. Guo, P.F.Shi, X. Q. Cheng and L. Sun. *Electrochim. Acta*. 54 (2009) 5796.
19. J.Cho, Y. J. Kim and B. Park. *Chem. Mater*. 12 (2000) 3788.
20. A. Schechter and D. Aurbach. *Langmuir*. 15 (1999) 3334.
21. R. Yazami. *Electrochimica Acta*. 45 (1999) 87.
22. H.D. Zhang, K.Q. Sun, Z. C. Feng, P. L. Ying and C. Li. *Appl. Catal., A*. 305 (2006) 110.
23. X.Y.Chen, X.Wang, C.H.An, J.W.Liu and Y.T.Qian. *Mater. Res. Bull.,* 40(2005) 469.
24. D. Arumugam and G. P. Kalaignan, *Electrochim. Acta.* 55 (2010) 8709.
25. L. Wang, J.S.Zhao, S.H.Guo, X.M. He, C.Y.Jiang and C.R. Wan, *Int. J. Electrochem. SC*.5(2010)1113.
26. M.D. Levi, G. Salitra, B. Markovsky, H. Teller, D. Aurbach, U. Heider and L. Heider. *J. Electrochem. Soc.,* 146 (1999) 1279.
27. H. W. Chan, J. G. Duh and S. R. Sheen. *Electrochim. Acta.* 51 (2006) 3645.